



Investigating agricultural drought in Northern Italy through explainable Machine Learning: Insights from the 2022 drought

Chenli Xue^{a,b}, Aurora Ghirardelli^b, Jianping Chen^a, Paolo Tarolli^{b,*}

^a School of Earth Sciences and Resources, China University of Geosciences, Beijing 100083, China

^b Department of Land, Environment, Agriculture and Forestry, University of Padova, Legnaro, PD 35020, Italy

ARTICLE INFO

Keywords:

Agricultural Drought Monitoring
Ensemble Learning
Explainable AI
Northern Italy
Shapley Additive Explanation

ABSTRACT

Agricultural drought is a complex natural hazard involving multiple variables and has garnered increasing attention for its severe threat to food security worldwide. In the context of climate change and the increased occurrence of drought events, it is crucial to monitor drought drivers and progression to plan the subsequent efforts in drought prevention, adaptation, and migration. However, previous studies on agricultural drought often focused on precipitation or evapotranspiration, overlooking other potential drivers related to crop drought stress. Additionally, macro-level analyses of drought-driving mechanisms struggle to reveal the underlying contexts of varying drought intensities. Northern Italy is one of the most important agricultural regions in Europe and is also a hotspot affected by extreme climate events in the world. In the summer of 2022, an extreme drought struck Europe once again, causing significant damage to the agricultural regions of Northern Italy. However, no studies to date have revealed the potential impacts and extent of extreme drought on this crucial agricultural area at a regional scale. Therefore, a comprehensive understanding of agricultural drought still requires further clarification and differentiated driver analysis. This study proposed a novel framework to comprehensively monitor agricultural drought with ensemble machine learning by constructing an integrated agriculture drought index (IADI) with remote sensing-related data including meteorology, soil, geomorphology, and vegetation conditions. Additionally, the Shapley Additive Explanation (SHAP) explainable model was applied to reveal the driving mechanism behind the drought event that occurred in northern Italy in the summer of 2022. Results indicated that the proposed explainable ensemble machine learning model with multi-source remote sensing products could effectively depict the evolution of agricultural drought with spatially continuous maps on an 8-day scales. The SHAP analysis demonstrated that the extreme and severe agricultural drought in the summer of 2022 was closely related to meteorological indicators especially precipitation and land surface temperature, which contributed 68.88% to the drought. Moreover, the new findings also highlighted that soil properties affected the agricultural drought with a contribution of 28.3%. Specifically, in the case of moderate and slight drought conditions, higher clay and soil organic carbon (SOC) content contribute to mitigating drought effects, while sandy and silty soils have the opposite effect, and the contributions from soil texture and SOC are more significant than precipitation and land surface temperature. The proposed research framework could effectively contribute to improving the methodology in agricultural drought research, potentially bringing more instructive insights for drought prevention and mitigation.

1. Introduction

Drought is a globally pervasive hazard with complex causative factors, and it can be categorized into multiple types based on various focal points, including meteorological, hydrological, agricultural, and ecological drought (Tarolli and Zhao, 2023). Among them, agricultural drought refers to the phenomenon in which insufficient soil moisture,

caused by various factors, adversely affects the normal growth and yield of crops. Due to its severe and direct threat to food security and socio-economic sustainable development, it has garnered widespread attention worldwide (Pan et al., 2023). More importantly, with the influence of global climate change, extreme weather events, such as heatwaves are becoming increasingly frequent (Arias et al., 2024). It has been reported that future climate would shift towards a drier trend, posing further

* Corresponding author.

E-mail address: paolo.tarolli@unipd.it (P. Tarolli).

threats to global agricultural production and water resource supply, particularly in the Mediterranean region (Wang et al., 2022). Therefore, it is urgent to accurately monitor and provide early warnings for regional agricultural drought, as well as to reveal its occurrence patterns and mechanisms.

Due to its inherent advantages of wide coverage and long-term observations, remote sensing has been frequently applied in regional agricultural drought monitoring. This involved analyzing information extracted from images related to vegetation, soil, and meteorological conditions, giving rise to numerous potential monitoring indices, such as the Temperature Rise Index (TRI) based on land surface temperature (Hu et al., 2020), the Normalized Difference Vegetation Index (NDVI) used for characterizing vegetation greenness, and the Standardized Precipitation Index (SPI) (Pan et al., 2023). Calculated based on a single indicator, the indices above are convenient for quick drought monitoring due to their simplicity and minimal data requirements. However, since they only consider single factors, they cannot accurately reflect the actual drought conditions in regions with diverse land covers, complex topography, and significant internal variations in geographic environments. Therefore, to comprehensively reflect drought conditions, remote sensing indices involving multiple indicators and considering their interrelationships have been further developed and applied, including the Standardized Precipitation Evapotranspiration Index (SPEI) derived from precipitation and evapotranspiration, vegetation health index (VHI) calculated from NDVI and land surface temperature (Javed et al., 2021), Temperature Vegetation Dryness Index (TVDI) based on standardized land surface temperature and vegetation index (Zhao et al., 2024), Palmer Drought Severity Index (PDSI) based on precipitation, temperature, potential evapotranspiration and soil parameters (Faiz et al., 2022). Furthermore, to address the inherent uncertainty in estimating drought severity based on a single index, some studies have also attempted to use composite indices and demonstrated their feasibility (Rossi et al., 2023). However, despite the significant convenience provided by these remote sensing-based methods for regional drought monitoring, they tend to focus more on meteorological and vegetation factors, overlooking the potential impacts of other factors, e.g. soil texture and soil organic content. Moreover, the subjective nature and regional variations in weight allocation during the process of combining multiple indices have also affected their performance in agricultural drought monitoring.

Realizing the importance of incorporating multisource data, an increasing number of researches have attempted to utilize multifaceted factors encompassing meteorological, soil and vegetation-related variables associated with drought occurrence, undertaking a series of explorations. Some researchers had constructed drought monitoring models by combining multiple linear regression with agricultural drought-related dataset (Zhang et al., 2022). However, these linear models may not effectively capture the complex relationships among multisource data, and they exhibited limitations when confronted with large volumes of data. To address these deficiencies, some approaches had been introduced into drought monitoring to enhance the model applicability and robustness. For example, Empirical Mode Decomposition (EMD) has been employed for the analysis of the formation and causes of agricultural drought due to its particular suitability for complex data with nonlinear and non-stationary characteristics with high flexibility (Jin et al., 2023). In addition, some local regression methods, such as Geographically Weighted Regression (GWR), have also been adopted for the construction of agricultural drought indices (Khosravi et al., 2024). Despite capturing the spatially heterogeneous features of drought through separate regressions at different locations, its fundamental nature remained a linear regression model. Machine learning is capable of handling high-dimensional, large-scale data and discovering correlations and patterns within them, thereby providing deeper insights. In recent years, with the rapid advancement of artificial intelligence, significant breakthroughs have been achieved in drought modeling and monitoring (Mardian et al., 2023). For instance, numerous

studies have attempted to utilize various machine learning methods to estimate drought probabilities using logistic regression, soil moisture estimation based on ensemble algorithms, short-term drought prediction through deep learning, and future drought projection by tree-based algorithms (Prodhan et al., 2022). However, most of these studies always utilized traditional meteorological drought indices such as SPI and SPEI in agricultural drought analysis. Furthermore, there was limited research that comprehensively utilized information from meteorology, vegetation, soil, and topography for multi-model learning in agricultural drought analysis. However, despite the ability of machine learning to enhance the accuracy of drought monitoring by leveraging large and diverse datasets, its black-box nature, which hinders the interpretability of the decisions made by the model, has been a subject of controversy (Mardian et al., 2023). Recently, the development of explainable machine learning has opened up opportunities for analyzing the driving mechanisms of agricultural drought by measuring the contribution of each feature to the output or prediction. Specifically, some global metrics and methods have been widely utilized for explaining decision-making in machine learning models, such as Mean Decrease in Impurity, Mean Decrease in Accuracy, and the Partial Dependence Plot (Friedman, 2001), failing to provide detailed decision criteria for specific observation. Recently, several local interpretation methods for machine learning models have been proposed to address this limitation. For example, Local Interpretable Model-agnostic Explanations (LIME) interprets predictions by generating virtual samples and employing simple models. However, its stability and consistency may be compromised, particularly when dealing with complex underlying models (Mardian et al., 2023). Compared to LIME, the recently proposed SHAP model, based on game theory, possesses a more rigorous mathematical foundation. It allows for both global and local explanations simultaneously and exhibits more stable and accurate results. Therefore, it is worthwhile to further address the potential limitations of existing agricultural drought monitoring and driving mechanism analyses exploring two main novel approaches: (1) integrating multi-source data related to agricultural drought and incorporating soil properties into ensemble learning models to monitor agricultural drought at a higher time resolution, considering the perspective of crop stress; (2) applying the latest interpretable machine learning techniques to reveal the differentiated driving mechanisms behind varying levels of agricultural drought, aiming to provide a more comprehensive understanding of the occurrence and development of agricultural drought.

Northern Italy, encompassing the Po Valley, stands as one of the most important agricultural production regions in Italy and even Europe. Simultaneously, it is also a hotspot for climate change (Straffellini and Tarolli, 2023). Research indicated that since the 1980s, the frequency of drought events in the Mediterranean and Europe had been gradually increasing, and drought in northern Italy had also become more prevalent (Baronetti et al., 2022). In the summers of 2011 and 2017, northern Italy experienced severe droughts, leading to soil moisture deficits in the region and ultimately resulting in reduced crop yields (García-Herrera et al., 2019). In the summer of 2022, another severe drought event swept through most parts of Europe, hitting the Po Valley with pronounced features of severe water scarcity and heatwaves (Bonaldo et al., 2023). It was reported to be a record-breaking drought event in the past two centuries, characterized by a dramatic drop in the Po River water level and a reduction in irrigation water supply (Montanari et al., 2023). Meanwhile, studies on future climate change indicated that the risk of drought in this region is expected to increase by 50%, and its impact is projected to rise by 80% (Sofia et al., 2023). Despite Northern Italy, a major agricultural region in Europe, experiencing extreme droughts driven by climate change, no study has yet comprehensively monitored agricultural drought at a regional scale or investigated the driving mechanisms behind the 2022 extreme drought event. Therefore, in this context, it is critically urgent to leverage more comprehensive data to achieve high spatiotemporal resolution of agricultural drought monitoring and unveil the underlying driving

mechanisms for agricultural drought prevention and food security. The aims of this study were as follows: (1) to construct a high temporal resolution model for agricultural drought monitoring by integrating ensemble machine learning and multi-source data, including meteorological, vegetation, soil, and topography. (2) to evaluate the applicability and effectiveness of the proposed Integrated Agricultural Drought Index (IADI) and analyze the evolution of the 2022 summer drought at an 8-day scale. (3) to reveal the underlying driving mechanisms behind different levels of agricultural drought and propose drought prevention measures. The findings of this study will provide a more comprehensive understanding of agricultural drought monitoring and contribute to a deeper insight into the occurrence mechanisms of agricultural drought.

2. Materials and methods

2.1. Study area

The investigated area, located in Northern Italy, mainly involves seven regions from Piemonte in the west to Veneto in the east, encompassing the entire Po Valley, covering an area of about 46,000 km² (Fig. 1). Encircled by mountains on three sides, there are expansive alluvial plains stretching from west to east. The agricultural system in the research area is predominantly irrigated (Valmassoi et al., 2020). In the plain, the main crops are maize, wheat, soybean, and rice. In steep-slope regions, agricultural types include vineyards, olive groves and orchards (d'Andrimont et al., 2021; European Environment Agency, 2019). Encompassing the largest plain regions in Italy with favorable geographical conditions, climate, and soil characteristics, the study area is a pivotal agricultural center in Italy for diverse agricultural activities, exerting a significant influence on food security and economic well-being.

However, with the influence of global climate change, the frequency and intensity of drought events have gradually increased across the European continent in recent years, posing significant risks to local agricultural development. Furthermore, intensified drought stress has also led to other issues, including saltwater intrusion and soil salinization which further worsening local agricultural production conditions (Tarolli et al., 2024). For example, an extreme heatwave struck Europe in the summer of 2022, resulting in a significant decrease in the water flow of the Po River. The ensuing severe drought led to reduced agricultural yields, causing substantial losses for local farmers. In light of this, to alleviate the impact of drought on agricultural production in Northern Italy, it is crucial to conduct a comprehensive analysis of drought events, monitor the occurrence trends, and reveal their underlying mechanisms.

2.2. Data sources and processing

The occurrence and impact processes of agricultural drought are determined by various triggering factors, involving not only meteorological information such as precipitation but also factors related to soil, vegetation status, and topography. This also forms the theoretical basis for constructing the comprehensive agricultural drought monitoring model. Therefore, to reveal the occurrence and development processes of agricultural drought, this study utilized multiple factors (Table. 1) related to agricultural drought over the spring-summer crop growing period (May to September) from 2015 to 2022 to construct an IADI calculated on the cropland extracted from CORINE Land Cover 2018. After evaluation, all input datasets were resampled to a spatial resolution of 250 m for subsequent analysis. On one hand, this retains the advantages of high-resolution data as much as possible; on the other hand, it ensures acceptable computational efficiency for the subsequent

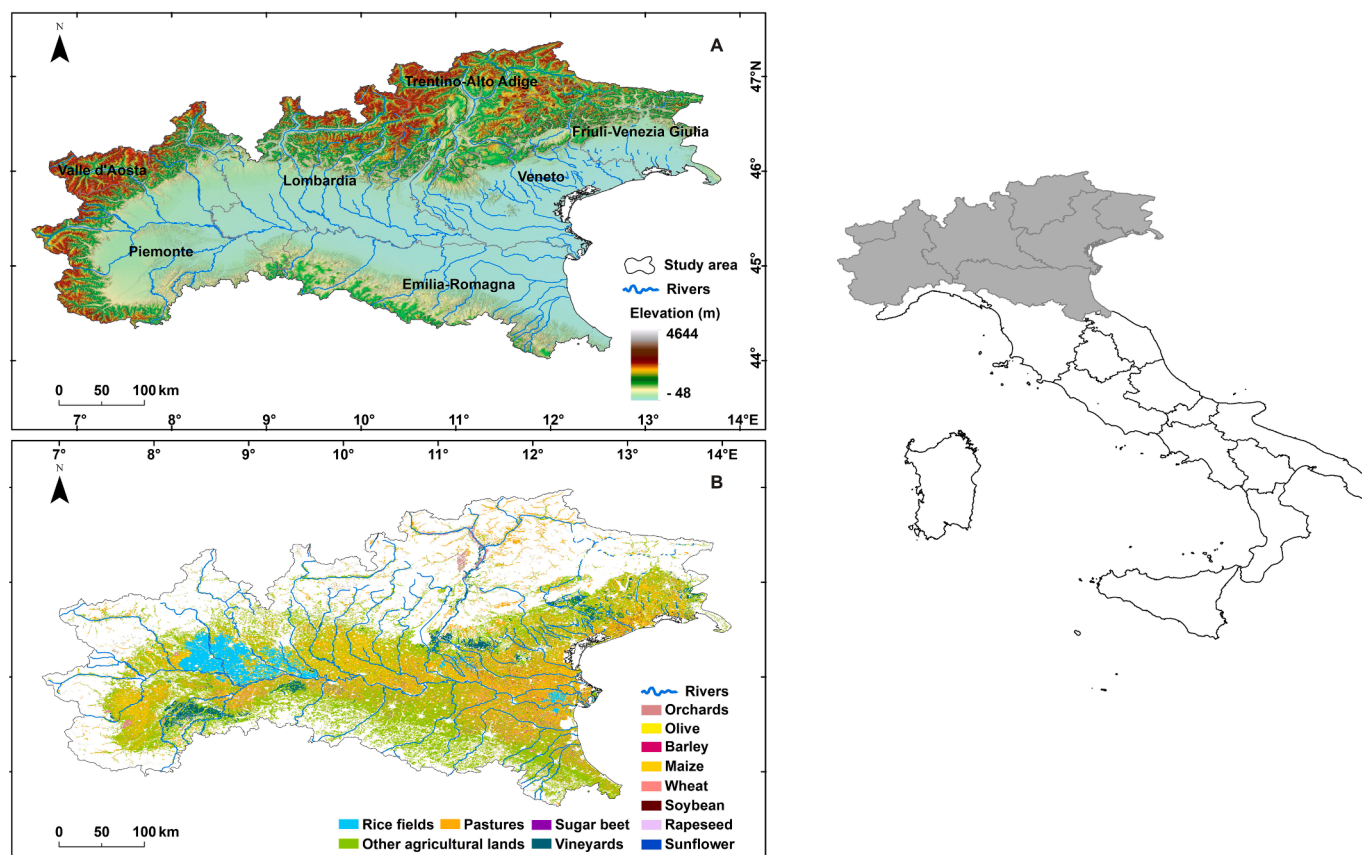


Fig. 1. Over view of the study area. A: Topography and hydrography, B: Main crop types from CORINE Land Cover vector and EUCROP, 2018 (Agency and Land Cover, 2018)

Table 1
Dataset utilized in the study.

Variables	Temporal Resolution	Spatial Resolution	Units	Sources
LST	8 Day	1.2 km	°C	https://lpdaac.usgs.gov/products/mod11a2v061/ (Wan et al., 2021)
ET	8 Day	500 m	mm	https://lpdaac.usgs.gov/products/mod16a2v061/ (Running et al., 2021)
PRE	Daily	0.05°	mm	https://data.chc.ucsb.edu/products/CHIRPS-2.0/ (Funk et al., 2015)
SIF	8 Day	0.05°	$W m^{-2} \mu m^{-1} sr^{-1}$	https://globalecology.unh.edu/ (Li and Xiao, 2019)
CLAY	–	250 m	g/kg	https://soilgrids.org/ (Batjes and Calisto, 2023)
SILT	–	250 m	g/kg	https://soilgrids.org/ (Batjes and Calisto, 2023)
SAND	–	250 m	g/kg	https://soilgrids.org/ (Batjes and Calisto, 2023)
SOC	–	250 m	dg/kg	https://soilgrids.org/ (Batjes and Calisto, 2023)
SM	Daily	1 km	%	https://land.copernicus.eu/global/products/ssm/ (Bauer-Marschallinger et al., 2019)
DEM	–	30 m	m	https://lpdaac.usgs.gov/products/nasadem_hgtv001/ (NASA JPL, 2020)

Notes: LST (land surface temperature); ET (evapotranspiration); PRE (precipitation); SIF (solar-induced chlorophyll fluorescence); SOC (soil organic carbon); SM (soil moisture).

training of machine learning models.

(1) Meteorological data

The 8-day land surface temperature (MOD11A2) in a 1200 x 1200 m grid and 8-day composite evapotranspiration (MOD16A2) at a 500-meter pixel resolution were obtained from the MODIS satellite products; The daily precipitation used in this study was from the CHIRPS dataset (Climate Hazards Group InfraRed Precipitation with Station Data) with a spatial resolution of 0.05°. To achieve the drought monitoring with high temporal resolution and maintain consistency with other meteorological data, the daily precipitation was computed as 8-day products through summation.

(2) Vegetation Data

The growth of crops and vegetation is directly affected by agricultural drought. Compared to indices such as NDVI that merely characterize vegetation greenness, some studies have found that Solar-induced chlorophyll fluorescence (SIF) products could reflect vegetation photosynthetic rates more in real-time and show closer correlations with plant physiological status (Liu et al., 2020). Therefore, the global GOSIF (OCO-2 SIF) product with 0.05° spatial and 8-day temporal resolutions was utilized in this research.

(3) Soil data

The SoilGrids version 2.0 product (250 m), including proportion of clay, silt, sand particles, and soil organic carbon content at 5 cm depth, was adopted to represent soil properties. Additionally, daily surface soil moisture with a 1 km resolution was collected from the Copernicus Global Land Service and then utilized to calculate its 8-day mean. Retrieved from the Sentinel-1 satellites, the soil moisture data had been validated with in-situ measurements and yielded high agreement over plains and agricultural areas in Italy (Bauer-Marschallinger et al., 2019).

(4) Topographic data

The NASADEM with a 30 m resolution was employed to represent the topographical information in this study.

2.3. Methodology

In this study, an explainable regression model based on the stacking strategy was trained to construct an IADI with higher spatiotemporal resolution compared to currently available indexes (Liu et al., 2020; Mardian et al., 2023), and then the mechanism behind drought events was analyzed. To construct the IADI, all predictor variables and the dependent variable (soil moisture) of the training set were used to train the four regression models. Subsequently, the model that performed the

best on the validation dataset was selected as the final predictive model due to its superior capability. Ranging from 0 to 1, the IADI would reflect the severity of agricultural drought, where lower values indicated a more severe drought condition. Based on the classification criteria for drought severity from previous studies (Liu et al., 2020), the agricultural drought was divided into nine categories according to the quantile method as follows: extremely dry (0.12–0.15), severe dry (0.15–0.23), moderate dry (0.23–0.25), slight dry (0.25–0.32), normal (0.32–0.38), slight wet (0.38–0.44), moderate wet (0.44–0.52), severe wet (0.52–0.63), extremely wet (0.63–0.79). The model with the best performance in the validation dataset would be adopted to produce the IADI maps. The overall research framework is illustrated in Fig. 2.

2.3.1. Stacking ensemble learning

In this study, different types of machine learning regression models including RandomForest, XGBoost, and CatBoost were trained. Random Forest Regression (RFR) is an ensemble learning method based on bagging strategy which combines the predictions of multiple decision trees, leveraging the power of both bagging and feature randomness to enhance predictive performance and mitigate overfitting. XGBoosting Regression (XGBR), proposed by Chen and Guestrin (Chen and Guestrin, 2016), belongs to the family of gradient boosting algorithms. It excels in regression tasks by sequentially boosting weak learners to refine the predictive model through the integration of a set of optimization techniques, regularization mechanisms, and parallel processing capabilities. Introduced by Ostroumova (Ostroumova et al., 2017), CatBoost Regression was designed to address tasks with categorical features. It also proposed a histogram-based method to improve the training efficiency. Additionally, regularization techniques such as automatic control of tree depth and feature-based splitting were also integrated in the algorithm to prevent overfitting.

The above algorithms, based on bagging and boosting approach, exhibit distinct advantages in terms of model performance improvement strategies and data processing methods. To combine the strengths of different algorithms, the stacking strategy was then employed to integrate the aforementioned three models. Serving as base learners, the outputs from the above models were used as inputs for training the second model to obtain the final *meta*-learner. Generally, a simple linear model such as Support Vector Machines (SVM) could be adopted as the second model to mitigate the risk of overfitting. In this study, the dataset was divided into two parts as training set (70 %, 38,523 points) for model training and the remaining 30 % (16511 points) was used for validation. Before training models, all predictor variables and the dependent variable (soil moisture) were normalized to enhance efficiency.

2.3.2. Explainability in machine learning

In this paper, taking the summer drought (2022) in northern Italy as an example, the SHapley Additive exPlanations (SHAP) analysis was employed to the ensemble machine learning model to calculate the

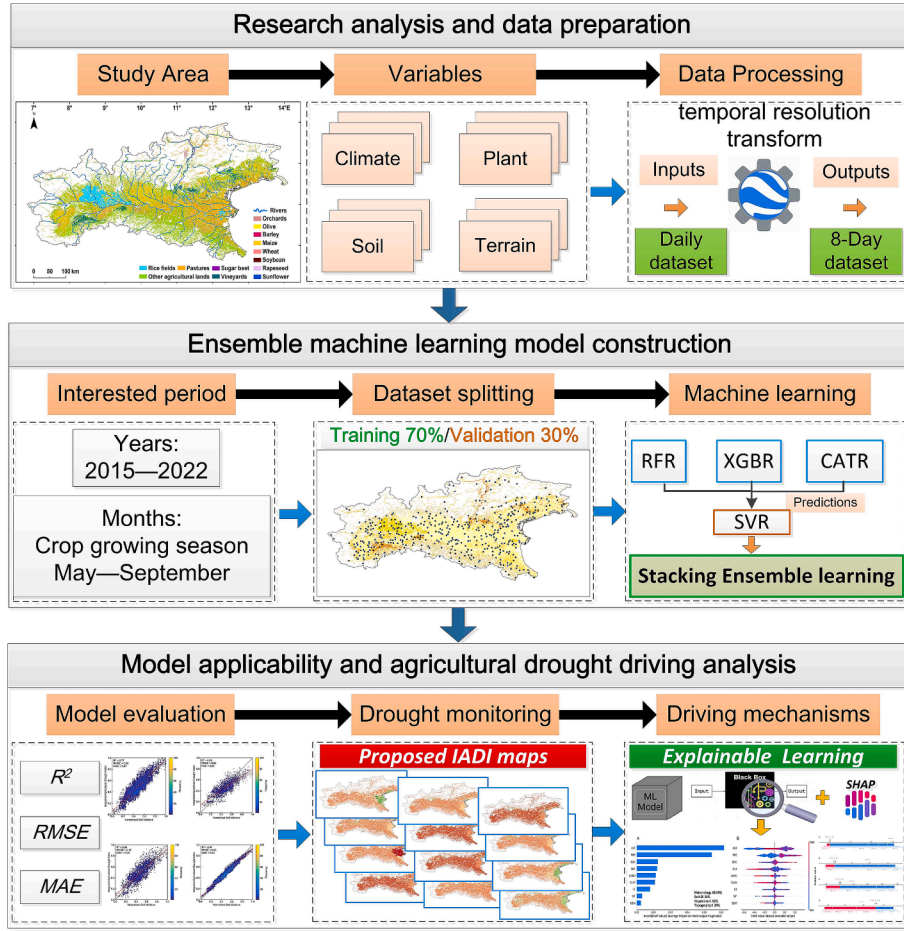


Fig. 2. Research framework Diagram.

global contributions of all predictor variables. In addition, different degrees of drought were selected as typical cases for local interpretation to unveil the underlying mechanisms behind the occurrence of agricultural drought.

Based on the cooperative game theory proposed by Shapley (Shapley, 1953), which aims to determine the relative contribution of each participant, the SHAP model has recently emerged as a powerful tool in the realm of explainable machine learning. It assigns the contribution of each feature to the final prediction through Shapley values, providing a unified framework for explaining the output of any machine learning model. The computation of Shapley values can be formulated as follows:

$$\phi_m(v) = \sum_{S \subseteq N \setminus \{m\}} \frac{|S|!(|N| - |S| - 1)!}{|N|!} (v(S \cup \{m\}) - v(S)) \quad (1)$$

where $\phi_m(v)$ is the contribution of feature m , N and S are the set and subset of all features, respectively. $v(S \cup \{m\})$ and $v(S)$ represent the model outputs in various feature combinations whether m is involved or not, respectively. The term $\frac{|S|!(|N| - |S| - 1)!}{|N|!}$ denotes the probability corresponding to various feature combinations. Therefore, the result obtained from the above expression represents the marginal contribution of feature m to the final outputs.

When it comes to the total contribution of all features for each observation, it could be expressed as follows:

$$g(x) = \phi_0 + \sum_{m=1}^M \phi_m z'_m \quad (2)$$

where M is the number of all features, and ϕ_0 represents the model outputs without any features.

2.3.3. Model evaluation

Utilizing 70 % of the whole data during vegetation growing seasons from 2015 to 2022, the three base models (RFR, XGBR, CATR) and the final meta-model were trained using the Bayesian Optimization method to select optimal hyperparameters. Compared to Grid Search and Random Search, Bayesian Optimization could utilize prior information to iteratively update the model, allowing for more intelligent selection of subsequent parameters. This significantly enhances computational efficiency while seeking optimal parameters (Pradhan et al., 2021). Subsequently, the trained regression models were validated using the remaining 30 % of the data, and their performance was evaluated through R^2 , Root Mean Squared Error (RMSE), and Mean Absolute Error (MAE) as follows:

$$R^2 = 1 - \frac{\sum_{i=1}^n (y_i - \hat{y}_i)^2}{\sum_{i=1}^n (y_i - \bar{y})^2} \quad (3)$$

$$RMSE = \sqrt{\frac{\sum_{i=1}^n (y_i - \hat{y}_i)^2}{n}} \quad (4)$$

$$MAE = \frac{\sum_{i=1}^n |y_i - \hat{y}_i|}{n} \quad (5)$$

where y_i , \hat{y}_i and \bar{y} represent the actual observed values, model predictions, and mean values of the actual observations, respectively. n denotes the total number of observations.

R^2 reflects the fitting level of the model to the actual observed values, while *RMSE* and *MAE* provide information about the predictive accuracy and error magnitude of the models. Compared to *MAE*, *RMSE* is more sensitive to outliers, and they focus on different aspects of the prediction error. The combination of them could provide a more comprehensive assessment of the model performance.

3. Results

3.1. Evaluation of drought monitoring performance for IADI

The performance of different regression models on the training and validation sets was shown in Table 2. It was observed that the RFR model performed the best on the training set but exhibited the poorest performance on the validation set, indicating its poor generalization performance. In comparison, the XGBR and CATR models showed similar performance on both the training and testing datasets. In general, the ensemble learning model (STACKING) exhibited the best performance on the validation dataset with a higher R^2 of 0.707 and lower errors ($RMSE = 0.088$, $MAE = 0.072$), leveraging the strengths of multiple models to enhance overall performance. Therefore, the ensemble machine learning model was ultimately adopted for constructing the IADI. After inputting multiband driving factor rasters into the model, time-series IADI maps were automatically generated.

Based on the well-trained ensemble learning model, multiband raster of all predictor variables at 8-day scales from different periods were then input into the model to predict the integrated agricultural drought index. As shown in Fig. 3, soil moisture and IADI in May 2022 in Northern Italy exhibited a generally consistent spatial pattern overall, but differences were also observed in local areas. This is primarily attributed to the limitations of the 8-day mosaic soil moisture products, where the mosaic results are constrained by data availability. In certain local areas, the mosaic results show significant discrepancies in soil moisture due to variations in meteorological conditions across different time periods. Specifically, compared to IADI, the soil moisture products exhibited significant data gaps attributed to the absence of satellite transit. In addition, noticeable striping patterns could be observed in the soil moisture data, resulting from the current limitation of satellite data, which cannot achieve daily coverage of the entire region. Consequently, the synthesized mosaic 8-day soil moisture products from different times were prone to such abrupt features, making it challenging to effectively capture the regional evolution characteristics of agricultural drought at 8-day scales.

3.2. Characteristics of the typical drought variations in 2022

As shown in Fig. 4, the detailed evolution characteristics of the 2022 Northern Italy extreme drought occurrence were captured by the IADI on an 8-day scale, providing spatially continuous results.

Table 2
Model Performance on the Training Set and Validation Set.

Model	Metrics	Training Set	Validation Set
RFR	R^2	0.958	0.659
	RMSE	0.033	0.100
	MAE	0.026	0.080
XGBR	R^2	0.764	0.671
	RMSE	0.077	0.092
	MAE	0.063	0.075
CATR	R^2	0.774	0.683
	RMSE	0.080	0.094
	MAE	0.070	0.077
STACKING	R^2	0.855	0.707
	RMSE	0.061	0.088
	MAE	0.049	0.072

Notes: RFR (Random Forest Regression); XGBR (XGBoost Regression); CATR (CatBoost Regression); STACKING (Ensemble learning model).

The IADI index revealed that a significant portion of agricultural areas in northern Italy had been subjected to agricultural drought disturbances starting from June, and then in the second week the drought conditions intensified and rapidly extended throughout the entire study area (Fig. 4). In the third week of June, most agricultural areas experienced another round of drought, with the Po River Delta (PRD) being particularly affected by extreme dry conditions. With the onset of precipitation in the last week of June, there was an alleviation of agricultural drought occurred in the PRD region where more precipitation occurred at that time. However, due to decreased precipitation, drought conditions in the central and western regions were further exacerbated. Throughout July, the study area experienced the most severe agricultural drought, with the entire region being affected by dry conditions. Starting from July, the agricultural drought resurged and reached its peak from the second week of July to the first week of August during this extreme heatwave event. During the two weeks in mid-July, most of the agricultural areas in northern Italy experienced severe or extremely severe drought conditions (Fig. 4). Then, in the fourth week of July, several rainfall events occurred in northern Italy, alleviating the agricultural drought to some extent. In the first two weeks of August, the agricultural regions were still grappling with drought, particularly in the central and western parts of the study area, where severe drought conditions persisted. However, in the following two weeks, the agricultural drought severity began to decrease, with the most noticeable alleviation observed in the Po River Delta in the eastern part, attributed to rainfall occurred in the PRD during this period (Fig. 4). The result is consistent with the existing literature (Straffellini and Tarolli, 2023) and it indicates that the IADI index is capable of monitoring the spatiotemporal evolution characteristics of agricultural drought at a higher temporal resolution with spatially continuous and reliable maps.

3.3. Contribution of different factors to drought

The global interpretative results of SHAP analysis were shown in Fig. 5 with the average SHAP values (Fig. 5A) for all predictor variables at each observation (Fig. 5B). It indicated that meteorological factors, including land surface temperature and precipitation, were the most crucial factors influencing the occurrence of widespread agricultural drought during the extreme heatwave event in the summer of 2022. Furthermore, the results also revealed that soil organic carbon and soil texture factors such as silt, sand, clay content also exerted a significant influence on the occurrence of agricultural drought, contributing notably at 28.3 % to the model output (Fig. 5A). In comparison, the influence from vegetation and topographic factors on the occurrence of this agricultural drought event was relatively small, with individual contributions of 1.62 % and 1.20 %, respectively.

Based on the entire training dataset, the SHAP global interpretative results could provide a comprehensive perspective on the attribution of the agricultural drought occurrence. However, the global results failed to deliver spatially heterogeneous information about the underlying driving mechanisms of agricultural drought because the causes of droughts may vary with different regions and degrees, each with its unique characteristics. Therefore, the local interpretive method of SHAP was further employed to analyze and interpret the causes of agricultural drought with diverse severity levels at different locations. As shown in Fig. 6, the local interpretive results for different severity levels of agricultural droughts were illustrated in the form of force plots.

The red color in the figure represented driving factors that could enhance the model outputs of the IADI, while the blue color indicated factors that would reduce the final results. Additionally, the length of the color bar represented the magnitude of their driving force for agricultural drought. The results indicated that for extreme and severe agricultural drought, meteorological factors including land surface temperature and precipitation were the predominant factors influencing their occurrence (Fig. 6A-6B). For moderate or slight agricultural drought conditions, the force plot reflected that higher clay content in

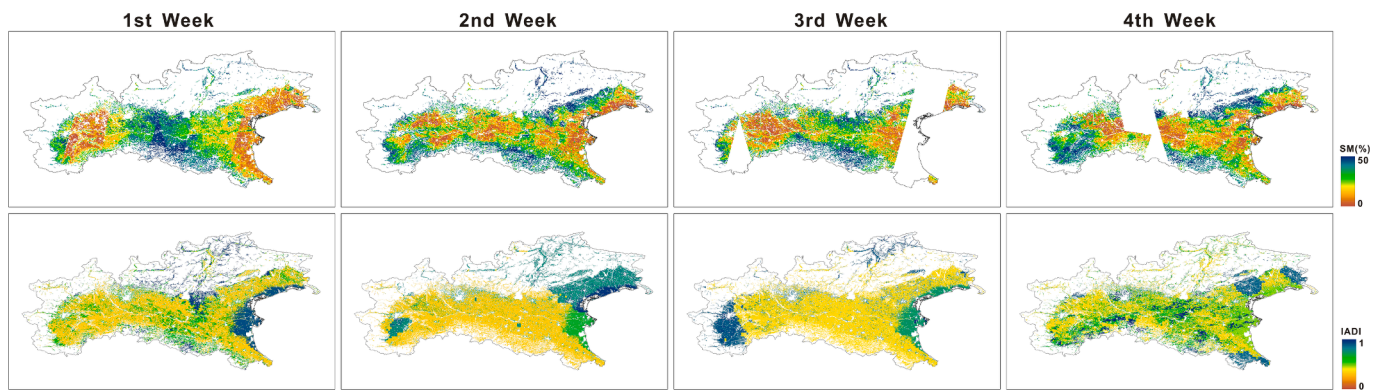


Fig. 3. Comparison of Soil Moisture and integrated agriculture drought index (IADI) in May 2022.

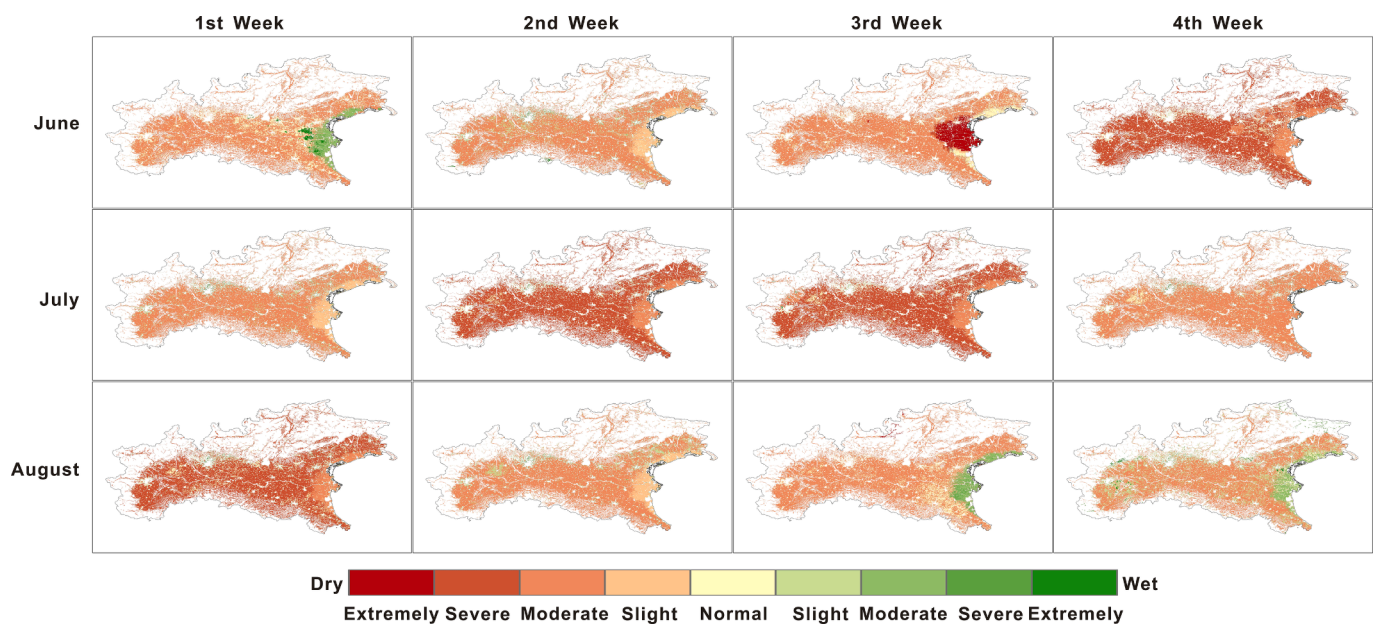


Fig. 4. Evolution of the agricultural drought occurrence during the summer of 2022 captured by integrated agriculture drought index (IADI).

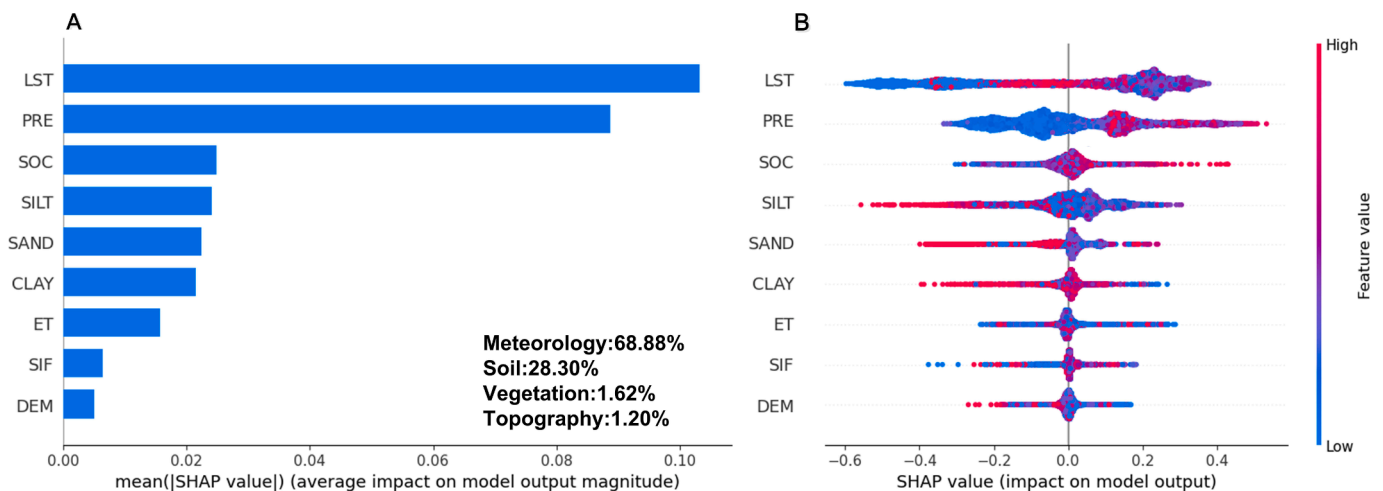


Fig. 5. Global interpretative results of SHAP analysis for the 2022 summer drought (LST: land surface temperature; PRE: precipitation; SOC: soil organic carbon; ET: evapotranspiration; SIF: solar-induced fluorescence).



Fig. 6. Force plots of SHAP analysis for the 2022 summer drought at different severity levels (A: Extreme Agricultural Drought; B: Severe Drought; C: Moderate/Slight Drought; D: Non-Drought) The red variable would increase the integrated agriculture drought index (IADI) value, while the blue one has the opposite effect. (For interpretation of the references to color in this figure legend, the reader is referred to the web version of this article.)

the soil would contribute to resisting the occurrence of drought, while sandy and silty soil, on the contrary, could reduce soil moisture content, leading to agricultural drought. Additionally, the results also depicted that regions with higher clay and soil organic carbon content were more conducive to soil moisture retention in response to precipitation, while sandy soil had negative impacts on preventing agricultural drought. For both moderate/slight and non-drought conditions, the influence of soil texture and soil organic carbon on agricultural drought was greater than that of meteorological factors, including land surface temperature, precipitation, and evapotranspiration (Fig. 6C-6D).

The SHAP analysis indicated that, for extreme and severe agricultural drought, precipitation and temperature predominantly influence the outcomes. For moderate/slight and non-droughts, it illustrated that soil texture and soil organic carbon also played a significant role and was even more important than meteorological factors. Specifically, excessively high levels of sandy and silty soil textures were detrimental to resisting drought, while clay and soil organic carbon were more favorable for soil moisture retention.

4. Discussion

4.1. The applicability of new drought index in northern Italy

At present, owing to its relatively high spatial-temporal resolution and extensive observational capabilities, satellite data is well-suited for surface soil moisture estimations across large regions even on global scales. For instance, the European Space Agency provides a daily surface soil moisture product derived from Sentinel-1 radar observations with reliable soil moisture estimates across Europe and the results had been validated in northern Italy (Bauer-Marschallinger et al., 2019). However, it cannot produce spatially continuous products with high temporal resolution due to the limitations imposed by satellite revisit cycle, which existed numerous data gaps within them (Paciolla et al., 2020). Taking the soil moisture, which could best characterize agricultural drought conditions, as the dependent variable, this study comprehensively integrated meteorological, soil, vegetation and topographical factors which potentially influencing soil moisture together, and input them into several machine learning models. As shown in Figs. 3 and 4, the predictive maps produced by the model with the optimal

performance revealed that the spatial pattern of the IADI index was generally consistent with the synthesized soil moisture, but the IADI exhibited a more continuous and complete spatio-temporal distribution. Actually, the soil moisture data used for model training is not an 8-day average but a mosaic of data collected over an 8-day period. Due to the limitations of the Sentinel-1 satellite's revisit cycle, it cannot fully cover the entire study area within 8 days. Therefore, the final 8-day mosaic is composed of soil moisture estimates from multiple dates stitched together. Therefore, due to challenges in achieving comprehensive coverage of the study area on an 8-day scales, the 8-day synthesized soil moisture existed shortcomings including spatial discontinuities, inconsistencies in adjacent ranges (Fig. 3) and low-precision estimations resulted from topography and vegetation coverage (Bauer-Marschalinger et al., 2019).

Combined large volume of multiple drivers with ensemble machine learning algorithms, the derived IADI implied the complex relationships among variables related to agricultural drought and could consistently provide spatially continuous agricultural drought monitoring results. The findings suggested that the integrated employment of potential factors affecting agricultural drought and machine learning was applicable for constructing a reliable agricultural drought monitoring system with a concise and rapid method.

4.2. Implications for agricultural development under drought

As depicted in Fig. 6, this study found that the predominant factors behind different severity levels of agricultural drought were distinct. In Fig. 6, red variables indicated that high values would lead to an improvement in agricultural conditions, representing decreased drought severity and risk. Conversely, blue variables could result in an exacerbation of IADI values, indicating more challenging agricultural conditions.

For extremely and severe agricultural drought, meteorological factors such as land surface temperature and precipitation were key determinants of its occurrence and development. Specifically, higher land surface temperatures would accelerate the evaporation process, leading to a reduction in soil moisture and conversely, the dry soil would also intensify the increase in land surface temperature (Tian et al., 2023). In addition, a novel finding of this study highlighted the significant role of soil texture and soil organic carbon in influencing agricultural drought, confirming that these parameters should not be overlooked, even on a regional scale. As presented in Fig. 5A, the contribution of soil texture and soil organic carbon to the final agricultural drought could reach up to nearly 30%. Previous experimental studies have also reported that soil texture strongly regulates soil moisture, especially during more frequent and prolonged droughts over Europe (Li et al., 2022). Specifically, to clarify the influence on soil moisture from texture, it has been demonstrated that soil available water in clay loam exhibited higher levels compared to sandy and silty soils through extensive field experiments. Generally, for different soil textures, the average, upper limit, and lower limit values of available water content are the highest in clay loam, then followed by silty and sandy soil (Salter and Williams, 1969). Soil particle size directly influenced soil pore structure, thereby affecting its water content. Soils with larger particles (sandy soil) are more prone to water infiltration but with poorer water retention capacity. By contrast, the clay particles are very small and tightly packed, resulting in overall strong impermeability and this means that clay can effectively prevent rapid infiltration and loss of water (Singh et al., 2017). However, empirical formulas for calculating plant available water content, developed based on extensive soil data, utilize both soil texture (proportions of sand, silt, and clay) and organic matter content to estimate soil water retention characteristics and have been widely applied (Saxton et al., 2006). In fact, the increase in organic matter content in the soil could facilitate the improvement of soil porosity and structure, mitigating the severity of compaction and thereby alleviating water scarcity (Sofia et al., 2023). Specifically, high content of soil organic

matter tends to generate more humic acids, facilitating its binding with mineral surfaces to form stable aggregates, thereby hindering the mineralization of organic carbon and promoting soil water retention (Sofia et al., 2023). Furthermore, humic acids can also create a water-retaining film, slowing down the rate of water evaporation, contributing to the reduction of moisture loss. On a regional scale, studies generally acknowledge the importance of soil texture in influencing soil water movement, leading to spatial variations in soil moisture evaporation, and other hydrological processes (Luan et al., 2024), but generally overlook the key role of SOC.

The force plots generated through SHAP analysis provide valuable insights into crucial parameters that should be considered before drought occurrences, facilitating hotspot identification based on local soil and meteorological conditions. For example, in areas with low soil organic carbon and clay content, targeted application of organic fertilizer can be employed to increase soil organic carbon and improve soil structure. Moreover, in these hotspot areas, potential drought trends detected during critical crop growth stages such as jointing, heading, and grain filling can be used to schedule irrigation in advance to mitigate damage to crops caused by drought stress (Deb et al., 2022). This practice contributes to enhancing soil fertility, boosting water retention capacity, and significantly benefiting agricultural drought resilience. These new findings can guide practical measures for farmers to implement daily water storage and drought prevention strategies based on local conditions. For example, in steep-slope agricultural systems near the Alps, the implementation of rainwater harvesting systems, such as micro-water storage in suitable locations, could be considered to achieve better water resource management (Wang et al., 2023). Additionally, critical areas could be identified based on local soil properties in advance for drought prevention. For example, to improve soil available water content, plowing can be conducted on drought-induced crusts in clay soils before potential precipitation, aiming to improve their water permeability. Additionally, soil structure and composition could be improved to mitigate water stress through conservation agriculture techniques such as cover crops, mulching and deep plowing (Luan et al., 2024; Tarolli and Zhao, 2023). In this key agricultural production area of Northern Italy, only a few studies have focused on the impact of drought on agriculture, and those that exist have primarily analyzed long-term historical drought trends and changes in drought severity under future climate scenarios (Montanari et al., 2023; Sofia et al., 2023). However, no research has explored the evolution and drivers of 2022 agricultural droughts. Our work integrated multi-source datasets related to agricultural drought and utilized interpretable machine learning to monitor drought on an 8-day timescale, providing insights into the driving mechanisms of drought and valuable guidance for agricultural development.

4.3. Uncertainties and future perspective

However, there were still some issues remained to be further investigated in this research. Firstly, the machine learning models could be further improved by inputting more accurate data. For instance, due to data availability, it was challenging to obtain sufficient in-situ data such as soil moisture, SOC, clay, silt, and sand at station scales and using data with coarser resolution would inevitably bring errors and increase the difficulty of exploring the complex relationships among datasets. In addition, the occurrence of agricultural drought is complex, and there is no consensus on the selection of its influencing factors. Secondly, the results of the SHAP analysis needed further on-site validation. On the one hand, the same model and identical input data may lead to different SHAP values in certain situations and this inconsistency could introduce uncertainties when interpreting the model. On the other hand, the interpretation of SHAP values may become more complex and unstable in the presence of highly non-linear relationships among data. While SHAP provided us with some insights into the underlying mechanisms of agricultural drought, due to its limitations, the final results needed to be

analyzed in conjunction with domain expertise and actual circumstances. Finally, the criteria for classifying the severity levels of agricultural drought still required further research. Although the percentile method was commonly adopted for categorizing different levels of drought, there was a lack of reliable theoretical basis behind it. Despite some limitations, the preliminary results could still aid in monitoring agricultural drought and deliver useful insights on understanding the complex mechanism.

5. Conclusions

In this study, a comprehensive research framework for monitoring agricultural drought and explaining its occurrence mechanism on a regional scale was proposed by integrating meteorological, vegetation, topographical and soil data with explainable ensemble machine learning models. Results indicated that the proposed IADI maps deduced from the ensemble learning model could effectively reflect the evolution of agricultural drought with spatially seamless results on an 8-day scales. The mechanisms of agricultural drought in the study area, a crucial agricultural region increasingly affected by extreme weather events, were primarily influenced by meteorological and soil factors, with contributions of 68.88 % and 28.30 %, respectively. More specifically, regarding different levels of agricultural drought, the extreme and severe drought were primarily controlled by land surface temperature and precipitation. In addition to meteorological factors, moderate and slight drought were also significantly influenced by soil properties, and regions with more clay loam and soil organic carbon were less prone to agricultural drought. Based on the above findings, some targeted measures were proposed for the agricultural drought prevention. The results could contribute with valuable insights for stakeholders such as farmers in drought management and provide potential prior knowledge for similar studies worldwide.

CRedit authorship contribution statement

Chenli Xue: Writing – original draft, Software, Methodology, Data curation, Conceptualization. **Aurora Ghirardelli:** Writing – review & editing, Validation. **Jianping Chen:** Writing – review & editing, Validation, Supervision. **Paolo Tarolli:** Writing – review & editing, Validation, Supervision, Project administration, Conceptualization.

Declaration of competing interest

The authors declare that they have no known competing financial interests or personal relationships that could have appeared to influence the work reported in this paper.

Acknowledgment

This study was carried out within the Agritech National Research Center and received funding from the European Union Next-GenerationEU (PIANO NAZIONALE DI RIPRESA E RESILIENZA (PNRR) – MISSIONE 4 COMPONENTE 2, INVESTIMENTO 1.4 – D.D. 1032 17/06/2022, CN00000022). This work was benefited by the China Scholarship Council (CSC) (Grant No. 202306400102) for supporting Chenli Xue's visiting scholar period at the University of Padova. This manuscript reflects only the authors' views and opinions; neither the European Union nor the European Commission can be considered responsible for them.

Data availability

Data will be made available on request.

References

- European Environment Agency. CORINE Land Cover 2018 (vector) [Data set]. European Environment Agency, 2019. 10.2909/71c95a07-e296-44fc-b22b-415f42acdf0.
- Arias, P.A., Rivera, J.A., Sörensson, A.A., Zachariah, M., Barnes, C., Philip, S., Kew, S., Vautard, R., Koren, G., Pinto, I., Vahlberg, M., Singh, R., Raju, E., Li, S., Yang, W., Vecchi, G.A., Otto, F.E.L., 2024. Interplay between climate change and climate variability: the 2022 drought in Central South America. *Clim. Change* 177, 6. <https://doi.org/10.1007/s10584-023-03664-4>.
- Baronetti, A., Dubreuil, V., Provenzale, A., Fratianni, S., 2022. Future droughts in northern Italy: high-resolution projections using EURO-CORDEX and MED-CORDEX ensembles. *Clim. Change* 172, 22. <https://doi.org/10.1007/s10584-022-03370-7>.
- Batjes, N.H., Calisto L., 2023. WoSIS-latest: Standardised world soil profile data. ISRIC Soil Data Hub resource identifier: <https://tinyurl.com/39xhaa9d>. Date downloaded: 15/08/2023.
- Bauer-Marschallinger, B., Freeman, V., Cao, S., Paulik, C., Schaufler, S., Stachl, T., Modanesi, S., Massari, C., Ciabatta, L., Brocca, L., Wagner, W., 2019. Toward global soil moisture monitoring with sentinel-1: harnessing assets and overcoming obstacles. *IEEE Trans. Geosci. Remote Sens.* 57, 520–539. <https://doi.org/10.1109/TGRS.2018.2858004>.
- Bonaldo, D., Bellafiore, D., Ferrarin, C., Ferretti, R., Ricchi, A., Sangelantoni, L., Vitelletti, M.L., 2023. The summer 2022 drought: a taste of future climate for the Po valley (Italy)? *Reg Environ Change* 23, 1. <https://doi.org/10.1007/s10113-022-02004-z>.
- Chen, T., Guestrin, C., 2016. XGBoost: A Scalable Tree Boosting System, in: Proceedings of the 22nd ACM SIGKDD International Conference on Knowledge Discovery and Data Mining. Presented at the KDD '16: The 22nd ACM SIGKDD International Conference on Knowledge Discovery and Data Mining, ACM, San Francisco California USA, pp. 785–794. 10.1145/2939672.2939785.
- d'Andrimont, R., Verhegghen, A., Lemoine, G., Kempeneers, P., Meroni, M., Van der Velde, M., 2021. From parcel to continental scale-A first European crop type map based on Sentinel-1 and LUCAS Copernicus in-situ observations. *Remote Sens. Environm.* 266, 112708. <https://doi.org/10.1016/j.rse.2021.112708>.
- Deb, P., Moradkhani, H., Han, X., Abbaszadeh, P., Xu, L., 2022. Assessing irrigation mitigating drought impacts on crop yields with an integrated modeling framework. *J. Hydrol.* 609, 127760. <https://doi.org/10.1016/j.jhydrol.2022.127760>.
- Faiz, M.A., Zhang, Y., Zhang, X., Ma, N., Aryal, S.K., Ha, T.T.V., Baig, F., Naz, F., 2022. A composite drought index developed for detecting large-scale drought characteristics. *J. Hydrol.* 605, 127308. <https://doi.org/10.1016/j.jhydrol.2021.127308>.
- Friedman, J.H., 2001. Greedy function approximation: a gradient boosting machine. *Ann. Stat.* 1189–1232.
- Funk, C., et al., 2015. The climate hazards infrared precipitation with stations—a new environmental record for monitoring extremes. *Sci. Data.* 2, 150066. <https://doi.org/10.1038/sdata.2015.66>.
- García-Herrera, R., Garrido-Perez, J.M., Barriopedro, D., Ordóñez, C., Vicente-Serrano, S.M., Nieto, R., Gimeno, L., Sorí, R., Yiou, P., 2019. The European 2016/17 Drought. *J. Clim.* 32, 3169–3187. <https://doi.org/10.1175/JCLI-D-18-0331.1>.
- Hu, T., Renzullo, L.J., Van Dijk, A.L.J.M., He, J., Tian, S., Xu, Z., Zhou, J., Liu, T., Liu, Q., 2020. Monitoring agricultural drought in Australia using MTSAT-2 land surface temperature retrievals. *Remote Sens. Environ.* 236, 111419. <https://doi.org/10.1016/j.rse.2019.111419>.
- Javed, T., Li, Y., Rashid, S., Li, F., Hu, Q., Feng, H., Chen, X., Ahmad, S., Liu, F., Pulatov, B., 2021. Performance and relationship of four different agricultural drought indices for drought monitoring in China's mainland using remote sensing data. *Sci. Total Environ.* 759, 143530. <https://doi.org/10.1016/j.scitotenv.2020.143530>.
- Jin, N., Shi, Y., Niu, W., He, L., 2023. Spatial and temporal patterns of agricultural drought in China during 1960–2020 characterized by use of the crop water deficit Abnormal Index. *J. Hydrol.* 627, 130454. <https://doi.org/10.1016/j.jhydrol.2023.130454>.
- Khosravi, Y., Homayouni, S., St-Hilaire, A., 2024. An integrated dryness index based on geographically weighted regression and satellite earth observations. *Sci. Total Environ.* 911, 168807. <https://doi.org/10.1016/j.scitotenv.2023.168807>.
- Li, H., Van Den Bulcke, J., Mendoza, O., Deroo, H., Haesaert, G., Dewitte, K., De Neve, S., Sleutel, S., 2022. Soil texture controls added organic matter mineralization by regulating soil moisture—evidence from a field experiment in a maritime climate. *Geoderma* 410, 115690. <https://doi.org/10.1016/j.geoderma.2021.115690>.
- Li, X., Xiao, J., 2019. A global, 0.05-degree product of solar-induced chlorophyll fluorescence derived from OCO-2, MODIS, and reanalysis data. *Remote Sens. (Basel)* 11, 517. <https://doi.org/10.3390/rs11050517>.
- Liu, X., Zhu, X., Zhang, Q., Yang, T., Pan, Y., Sun, P., 2020. A remote sensing and artificial neural network-based integrated agricultural drought index: Index development and applications. *Catena* 186, 104394. <https://doi.org/10.1016/j.catena.2019.104394>.
- Luan, Q., Gu, P., Sun, Q., Lai, B., Zhou, Y., Weng, B., 2024. Agricultural drought evaluation based on a soil moisture index coupled hydrological model in North China Plain. *Ecol. Ind.* 166, 112473. <https://doi.org/10.1016/j.ecolind.2024.112473>.
- Mardian, J., Champagne, C., Bonsal, B., Berg, A., 2023. A machine learning framework for predicting and understanding the canadian drought monitor. *Water Resour. Res.* 59. <https://doi.org/10.1029/2022WR033847> e2022WR033847.
- Montanari, A., Nguyen, H., Rubineti, S., Ceola, S., Galelli, S., Rubino, A., Zanchettin, D., 2023. Why the 2022 Po River drought is the worst in the past two centuries. *Sci. Adv.* 9, eadg8304. <https://doi.org/10.1126/sciadv.adg8304>.

- NASA JPL, 2020. NASADEM Merged DEM Global 1 arc second V001 . NASA EOSDIS Land Processes Distributed Active Archive Center. Accessed 2024-03-21 from 10.5067/MEaSUREs/NASADEM/NASADEM_HGT.001.
- Ostroumova, L., Gusev, G., Vorobev, A., Dorogush, A.V., Gulina, A., CatBoost: unbiased boosting with categorical features. *Neural Information Processing Systems*. <https://doi.org/10.48550/arXiv.1706.09516>.
- Paciolla, N., Corbari, C., Al Bitar, A., Kerr, Y., Mancini, M., 2020. Irrigation and Precipitation Hydrological Consistency with SMOS, SMAP, ESA-CCI, Copernicus SSM1km, and AMSR-2 Remotely Sensed Soil Moisture Products. *Remote Sens. (Basel)* 12, 3737. <https://doi.org/10.3390/rs12223737>.
- Pan, Y., Zhu, Y., Lü, H., Yagci, A.L., Fu, X., Liu, E., Xu, H., Ding, Z., Liu, R., 2023. Accuracy of agricultural drought indices and analysis of agricultural drought characteristics in China between 2000 and 2019. *Agric Water Manag* 283, 108305. <https://doi.org/10.1016/j.agwat.2023.108305>.
- Pradhan, B., Sameen, M.I., Al-Najjar, H.A.H., Sheng, D., Alamri, A.M., Park, H.-J., 2021. A Meta-Learning Approach of Optimisation for Spatial Prediction of Landslides. *Remote Sens. (Basel)* 13, 4521. <https://doi.org/10.3390/rs13224521>.
- Pradhan, F.A., Zhang, J., Pangali Sharma, T.P., Nanzad, L., Zhang, D., Seka, A.M., Ahmed, N., Hasan, S.S., Hoque, M.Z., Mohana, H.P., 2022. Projection of future drought and its impact on simulated crop yield over South Asia using ensemble machine learning approach. *Sci. Total Environ.* 807, 151029. <https://doi.org/10.1016/j.scitotenv.2021.151029>.
- Rossi, L., Naumann, G., Gabellani, S., Cammalleri, C., 2023. A combined index to characterize agricultural drought in Italy at municipality scale. *J. Hydrol.: Reg. Stud.* 47, 101404. <https://doi.org/10.1016/j.ejrh.2023.101404>.
- Running, S., Mu, Q., Zhao, M. (2021). MODIS/Terra Net Evapotranspiration 8-Day L4 Global 500m SIN Grid V061 < . NASA EOSDIS Land Processes Distributed Active Archive Center. Accessed 2024-03-21 from 10.5067/MODIS/MOD16A2.061.
- Salter, P.J., Williams, J.B., 1969. The influence of texture on the moisture characteristics of soil: V. relationships between particle-size composition and moisture contents at the upper and lower limits of available-water. *J. Soil Sci.* 20, 126–131. <https://doi.org/10.1111/j.1365-2389.1969.tb01561.x>.
- Saxton, K.E., Rawls, W.J., 2006. Soil Water Characteristic Estimates by Texture and Organic Matter for Hydrologic Solutions. *Soil Sci. Soc. Am. J.* 70 (5), 1569–1578. <https://doi.org/10.2136/sssaj2005.0117>.
- Shapley, L., 1953. A value for n-person games. In: Kuhn, H.W., Tucker, A.W. (Eds.), *Contributions to the Theory of Games (AM-28)*, Vol. II. Princeton University Press, pp. 307–317. <https://doi.org/10.1515/9781400881970-018>.
- Singh, M., Sarkar, B., Biswas, B., Bolan, N.S., Churchman, G.J., 2017. Relationship between soil clay mineralogy and carbon protection capacity as influenced by temperature and moisture. *Soil Biol. Biochem.* 109, 95–106. <https://doi.org/10.1016/j.soilbio.2017.02.003>.
- Sofia, G., Zaccone, C., Tarolli, P., 2023. Agricultural drought severity in NE Italy: Variability, bias, and future scenarios. *Int. Soil Water Conserv. Res.* S2095633923000576. <https://doi.org/10.1016/j.iswcr.2023.07.003>.
- Straffelini, E., Tarolli, P., 2023. Climate change-induced aridity is affecting agriculture in Northeast Italy. *Agr. Syst.* 208, 103647. <https://doi.org/10.1016/j.agsy.2023.103647>.
- Tarolli, P., Luo, J., Park, E., Barcaccia, G., Masin, R., 2024. Soil salinization in agriculture: Mitigation and adaptation strategies combining nature-based solutions and bioengineering. *iScience* 27,2,108830. [10.1016/j.isci.2024.108830](https://doi.org/10.1016/j.isci.2024.108830).
- Tarolli, P., Zhao, W., 2023. Drought in agriculture: Preservation, adaptation, migration. *TIG* 1, 100002. <https://doi.org/10.59717/j.xinn-geo.2023.100002>.
- Tian, J., Lu, H., Yang, K., Qin, J., Zhao, L., Jiang, Y., Shi, P., Ma, X., Zhou, J., 2023. Improving surface soil moisture estimation through assimilating satellite land surface temperature with a linear SM-LST relationship. *IEEE J. Sel. Top. Appl. Earth Observations Remote Sensing* 16, 7777–7790. <https://doi.org/10.1109/JSTARS.2023.3305888>.
- Valmassoi, A., Dudhia, J., Di Sabatino, S., Pilla, F., 2020. Evaluation of three new surface irrigation parameterizations in the WRF-ARW v3.8.1 model: the Po Valley (Italy) case study. *Geosci. Model Dev.* 13, 3179–3201. <https://doi.org/10.5194/gmd-13-3179-2020>.
- Wan, Z., Hook, S., Hulley, G. (2021). MODIS/Terra Land Surface Temperature/Emissivity 8-Day L3 Global 1km SIN Grid V061 . NASA EOSDIS Land Processes Distributed Active Archive Center. Accessed 2024-03-21 from 10.5067/MODIS/MOD11A2.061.
- Wang, W., Pijl, A., Tarolli, P., 2022. Future climate-zone shifts are threatening steep-slope agriculture. *Nat Food* 3, 193–196. <https://doi.org/10.1038/s43016-021-00454-y>.
- Wang, W., Straffelini, E., Tarolli, P., 2023. Steep-slope viticulture: The effectiveness of micro-water storage in improving the resilience to weather extremes. *Agric Water Manag* 286, 108398. <https://doi.org/10.1016/j.agwat.2023.108398>.
- Zhang, Y., Liu, X., Jiao, W., Zhao, L., Zeng, X., Xing, X., Zhang, L., Hong, Y., Lu, Q., 2022. A new multi-variable integrated framework for identifying flash drought in the Loess Plateau and Qinling Mountains regions of China. *Agric. Water Manag.* 265, 107544. <https://doi.org/10.1016/j.agwat.2022.107544>.
- Zhao, J., Peng, H., Yang, J., Huang, R., Huo, Z., Ma, Y., 2024. Response of winter wheat to different drought levels based on Google Earth Engine in the Huang-Huai-Hai Region China. *Agric Water Manag* 292, 108662. <https://doi.org/10.1016/j.agwat.2023.108662>.